Int. J. Electrochem. Sci., 11 **(2016)** 1293 - 1309

International Journal of
ELECTROCHEMICAL
SCIENCE
www.electrochemsci.org

Corrosion Mechanism of Low Alloy Steel in NaCl Solution with CO_2 and H_2S

Hongwei Wang[1,3,*], *Ping Zhou*[2], *Shaowen Huang*[2], *Chi Yu*[3]

[1] School of Information Science & Engineering, Northeastern University, Shenyang 110819, China
[2] Laiwu Iron and Steel Group Company Limited, Laiwu 271100, China
[3] Northeastern University at Qinhuangdao, Qinhuangdao 066004, China
[*]E-mail: wanghw0819@163.com

Received: 10 October 2015 / *Accepted:* 25 November 2015 / *Published:* 1 January 2016

The corrosion mechanism of low alloy steel is studied in NaCl solution containing CO_2 and H_2S. The study is carried out using accelerated corrosion and electrochemical measurements. Scanning electron microscopy (SEM) is applied to reflect the microstructure and corrosion morphology, and the compositions are analyzed using energy-dispersive spectroscopy (EDS) and X-ray diffraction (XRD). Results show the FeS and $FeCO_3$ are observed when corrosion immersion time is at 24h and 48h, an inner layer is relatively thin and a wavy outer layer is seen on the metal surface. From 96h to 288h, the pattern of $FeCO_3$ is not appeared, the thickness of outer layer and inner layer increase gradually, the corrosion products films are more uniform and dense. The experiments prove that the properties of corrosion product film seriously influence on corrosion resistance of low alloy steel.

Keywords: Low alloy steel; CO_2/H_2S; Accelerated corrosion; Electrochemical; Corrosion mechanism

1. INTRODUCTION

The corrosion resistance of alloy steel for petroleum industry with considerable amount of CO_2 and H_2S has always attracted more attention [1-4]. The special work conditions will bring disastrous accident and great financial loss. At present, the protective measures for metal corrosion in some sour environments mainly include: the anti-corrosion coating, corrosion inhibitor and corrosion resistant steel [5]. The coating and inhibitor can play a strong role, but the long-term cost will be very high, they may be unreliable, especially under the environment of high temperature and pressure. In many situations, the preferred alternative in terms of life-cycle economy and safety is the use of corrosion resistant steel. So it is important to develop alloy steel and investigate the corrosion mechanism.

Recently, the corrosion property of alloy steel under CO_2/H_2S coexistence environment has been widely researched and obtained some results. With the development of oil field with high H_2S content, the service environment is becoming worse and worse, the corrosion behavior under high partial pressure of H_2S is still poorly understood. Pots *et al*. [6] proposed a critical ratio of P_{CO_2}/P_{H_2S} to understand the corrosion behavior of alloy steel, and the reasons of corrosion products transformation are analyzed. Li et al. [2] have researched the corrosion properties of tubing steel under low CO_2/H_2S content environment and the results indicate that the H_2S has an important influence on the whole corrosion process and precipitation of iron sulfide on the steel surface is superior to iron carbonate. Zhao et al. [7] have studied that the corrosion behavior about Ni-based alloys in simulation solution containing CO_2/H_2S at different temperature. Wang et al. [8] have investigated the effects of alloy elements Cr on corrosion resistance in CO_2/H_2S environment. Their studies on the CO_2/H_2S corrosion are focused on the structure of corrosion scales using weight loss method.

Yet, the corrosion mechanism of alloy steel is an electrochemical process. The technology has been extensively applied to study the corrosion behavior [9-14]. Some achievements are obtained, mainly for single CO_2 [15-17] or H_2S environment [18-20]. However, very few studies under the CO_2/H_2S coexistence conditions are reported [21-24]. The electrochemical behaviors of low alloy steel during early corrosion stage are investigated [21, 23]. Wu et al [22] study the corrosion behavior of P110 grade tube steel after immersion 30 days. It is worth noting that most of the studies are performed to investigate corrosion properties at some point, and the corrosion mechanism of alloy steel under the different immersion period is seldom reported.

In this paper, the corrosion behaviors of alloy steel are studied under 3.5 wt% NaCl solution containing CO_2/H_2S coexistence conditions. The corrosion characteristics are analyzed by accelerated corrosion and electrochemical tests. The morphology and composition of the corrosion product film are characterized by scanning electron microscopy (SEM), energy dispersive spectrometer (EDS) and X-ray diffraction (XRD). These results would provide the theoretical support to develop corrosion resistant steel and its protection from CO_2 and H_2S corrosion.

2. EXPERIMENTAL

2.1 Material

The chemical composition of studied steel is shown in Table 1.

Table 1. Chemical composition of studied steel (wt %)

C	Si	Mn	P	S	Al	Cr	Cu	Ti	Mo	Ni	Nb	Fe
0.055	0.21	1.26	0.007	0.002	0.04	0.27	0.16	0.02	0.21	0.11	0.032	balance

2.2 Weight loss tests

The materials melted by a vacuum furnace are rolled into 12 mm from 110 mm. The rolling parameters are given including final rolling temperature for 825℃, final cooling temperature for 687℃, cooling rate for 5.3℃/s. All samples are cut into 25 mm × 20 mm × 4 mm. Before the test, the surfaces of the samples are polished with grit silicon papers progressively up to 1500 grade, a hole is machined with a diameter of 3mm in order to position the coupons, then degreased with acetone and rinsed with absolute alcohol, dried by the air and finally weighted. The corrosion test is carried out through high temperature and high pressure autoclave with 5L volume. The test electrolyte is 3.5 wt.% NaCl solution, pure nitrogen is bubbled into the electrolyte for 5h to deoxygenate. During the test, the solution is heated to 75 ^{o}C and the total pressure is set to 1.2 MPa with partial pressure 0.09 MPa H_2S, 0.64 MPa CO_2 and 0.47 MPa N_2. Five immersion times of 24h, 48h, 96h, 192h and 288h are chosen to investigate the corrosion behavior. After corrosion tests, the immerged specimens are immediately cleaned with distilled water and alcohol respectively. The chemical method with the etching solution compositions of 50 ml 37% HCl, 5g hexamethy lenetebramine (urotropine) and 450 ml deionized water is chosen to descale the scale, dried by the air and finally weighted. In every test, the three parallel samples are removed from the autoclave and rinsed with deionized water, and the mean value is obtained and the corrosion rate (v) is calculated according to the following equation [25]

$$v = \frac{8.76 \times 10^4 \times \Delta m}{S \times t \times \rho} \quad (1)$$

where v is the average corrosion rate, mm/year, Δm is the weight loss, g; S is the exposed surface area of samples, cm^2; t is the immersion duration, h; ρ is the density of tested metal.

2.3 Electrochemical measurements

The samples are machined into 10mm×10mm×3mm, and the area of exposed to the solution is 10mm×10mm, all other surfaces are embedded with epoxy resin. Prior to experiment, exposed surface are polished with grit silicon papers progressively up to 1500 grade. After weight loss tests, the specimens are removed from autoclave, and rinsed with deionized water, and used to finish the electrochemical tests. The electrochemical tests are performed with PATSTAT2273 workstation. A conventional three-electrode cell is used for the polarization curve and electrochemical impedance spectroscopy experiments. A platinum electrode is used as the auxiliary electrode, a saturated calomel electrode (SCE) is used as the reference electrode, and the sample is used as the working electrode. All polarization curve tests are conducted at a scan rate of 1mV/s. Each test is performed thrice to guarantee precision of experimental results and the CorrWiew software is applied to analyze the polarization curves. The electrochemical impedance spectroscopy measurements are performed using alternating current voltage amplitude of 8mV at open circuit voltage with frequencies ranging from 10^5 Hz to 0.1 Hz, and EIS results is analyzed by the Zsimpwin software. The tests are carried out in 3.5 wt% NaCl containing mixed gas H_2S, CO_2 and N_2 (1:7:5), the solution temperature is kept at 75 ^{o}C, the pH of the corrosion solution is 4.2.

2.4 Morphology observation

The microstructures are seen by optical microscope (OM) and scanning electron microscopy (SEM), the high-resolution transmission electron microscope (TEM) is used to reveal the microstructure in detail. After corrosion tests, the surface morphologies are observed by SEM, corrosion phases are detected by using X-ray diffraction (XRD) with Co Kα radiation and identified by matching peak positions automatically with MDI Jade software.

3. RESULTS AND DISCUSSION

3.1 Microstructure

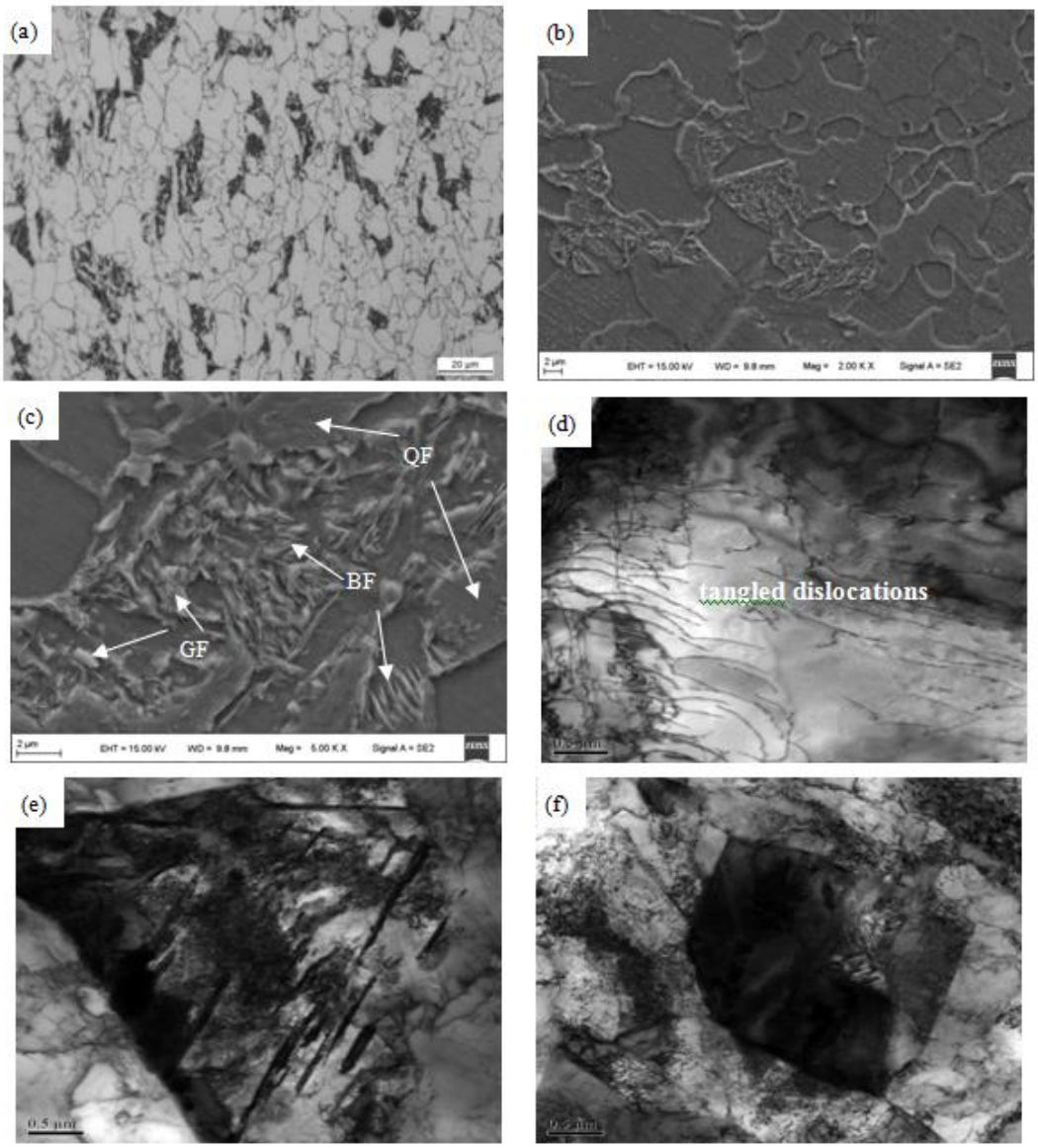

Figure 1. Microstructure characterization of studied steel showed by (a) OM; (b, c) SEM; (d, e, f) TEM

Fig.1 shows the microstructures of experimental steel. As can be seen from the Fig.1 (a) and Fig.1 (b), the type of microstructures is acicular ferrite (AF), ie., quasi polygonal ferrite (QF), granular bainitic ferrite (GF), and even a little banite ferrite (BF) [26]. The SEM and TEM are utilized to investigate the microstructure in detail. The SEM figure (Fig.1(c)) demonstrates that the QF, GF and BF. TEM figures (Fig.1(d)) displays non-parallel ferrite laths with high density of tangled dislocations, and the Fig.1(e, f) show the AF, which is consistent with OM and SEM observations.

3.2 Average corrosion rate

The relationships between weight loss and immersion time are shown in Fig.2. It is seen that the mass loss is also changed for studied steel after different immersion time. Weight loss exhibits three stages. It rises quickly at the beginning, and then increases stably, finally reaches a platform. At the first stage (0 h to 48 h), weight loss increases sharply from 0 to 9.9706 mg/cm^2. At middle stage, the weight loss increment is low. After immersion 192 h, the weight loss trends to be stable.

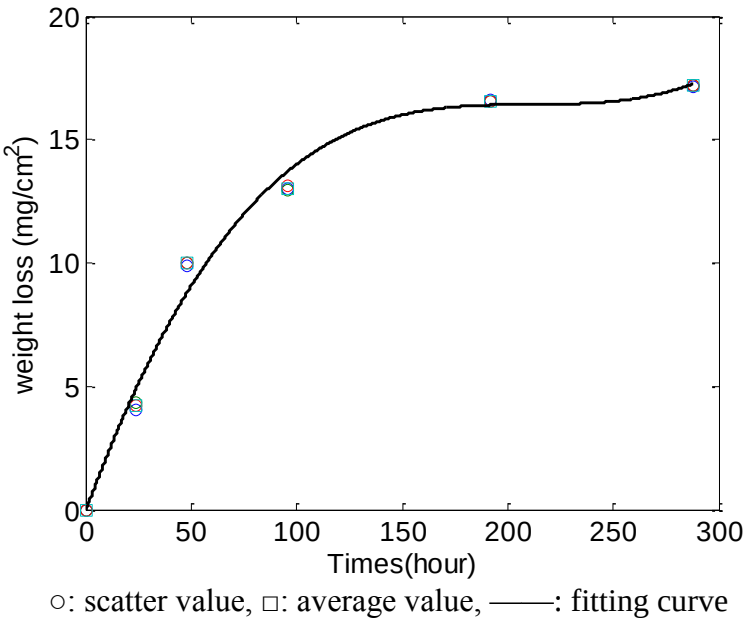

Figure 2. weight loss curve of studied steel

The polynomial fitting equation for weight loss and immersion time could be expressed as follows:

$$Y = 1.74\times10^{-6}t^3 - 0.001102t^2 + 0.2332t - 0.06368 \quad (2)$$

where t is immersion time (h) and the Y is the weight loss (mg/cm^2). The mass loss is much more, which mean that the corrosion rate is higher, it is the probable to appear the serious local corrosion or pitting corrosion phenomena. The average corrosion rates are calculated based on equation (1), the results are 1.936 2.298 1.501 0.955 and 0.660 mm/year for immersion 24, 48, 96, 192 and 288 h, respectively. It demonstrates the corrosion rate increases firstly and then decreases. The

transition point in the corrosion process is 48h, it is mainly related to the properties of corrosion product layer.

3.3 Electrochemical measurements

3.3.1 Potentiodynamic polarization curve analysis

The polarization curve measurements are perceived to be an effective ways which indicates the transient electrochemical corrosion process. Some important parameters are obtained by the experimental curves. The typical polarization curves of studied steel in CO_2 and H_2S solution after different immersion time 24, 48, 96, 192 and 288 h are shown in Fig.3. The electrochemical fitting parameters such as anodic and cathodic Tafel slopes (ba, bc), corrosion potential (E_{corr}), corrosion current densities (I_{corr}), polarization resistance (Rp) and corrosion rate (V) are obtained by extrapolation of Tafel lines, and fitting data are shown in Table2. It is found that the corrosion current density increases firstly and then decreases. In the early stages (24h to 48h), the the average corrosion current density increases from 0.1828 to 0.2030 mm/year, then decreases simultaneously with the increase immersion time from 48 h to 288 h. The average corrosion rates of studied steel after different immersion time 24, 48, 96, 192 and 288 h are 2.114, 2.408, 1.601, 1.110 and 0.734 mm/year, respectively. The smallest corrosion rate is observed at 288 h and the largest one is observed at 48h, which is in coincidence with the results of accelerated corrosion tests. From the polarization curves, it is seen that the cathodic shape of the curves changes greatly with the increase immersion time, which shows H_2S corrosion basically is related to cathodic reaction rate. The shape of the anodic portion and anodic reaction rate basically unchanged, which shows the corrosion process have little effect on anodic process. And the change trend of both the cathodic Tafel slopes and corrosion rate is consistent, the largest value is appeared at 48h.

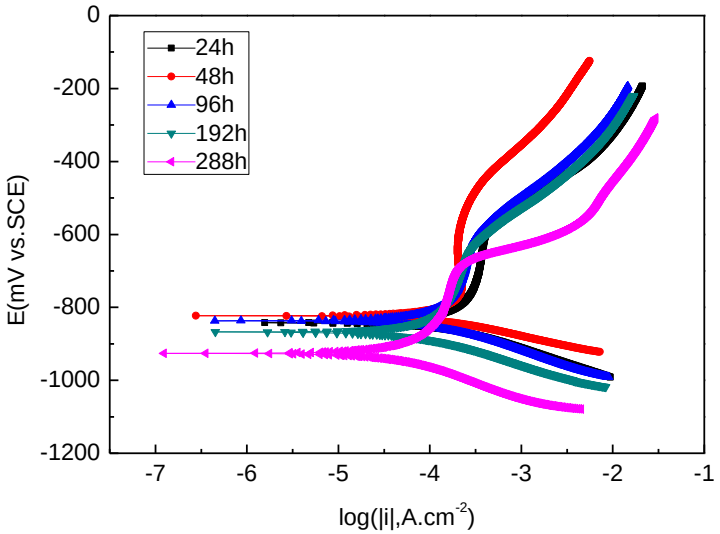

Figure 3. Potentiodynamic polarization curves of studied steel in CO_2/H_2S solution after different immersion time

Table 2. Potentiodynamic polarization parameters obtained from the anodic and cathodic polarization of studied steel after different immersion time in CO_2/H_2S solution

Immersion time/hour	Sample no.	ba (mV/dec)	bc (mV/dec)	E_{corr} (mV vs.SCE)	I_{corr} ($mA.cm^{-2}$)	Rp ($\Omega.cm^2$)	V (mm/year)
24h	1	136	-108	-841	0.1865	140	2.179
	2	145	-127	-855	0.1794	164	2.058
	3	130	-136	-859	0.1824	151	2.104
48h	1	98	-156	-822	0.2027	129	2.369
	2	105	-102	-834	0.2043	115	2.501
	3	116	-135	-828	0.2021	134	2.354
96	1	182	-90	-836	0.1320	198	1.543
	2	184	-101	-846	0.1540	184	1.601
	3	176	-105	-852	0.1587	180	1.658
192	1	260	-78	-867	0.0987	264	1.153
	2	228	-88	-869	0.0964	286	1.112
	3	181	-80	-891	0.0816	295	1.065
288	1	233	-81	-925	0.0515	507	0.602
	2	226	-75	-918	0.0598	409	0.789
	3	242	-78	-939	0.0704	364	0.812

3.3.2 Electrochemical impedance spectroscopy (EIS) analysis

The merits of EIS are able to get corrosion information that happen on the electrode surface. In order to better understand the influence of immersion time on the corrosion performance, the electrochemical impedance spectroscopy (EIS) is carried out under the same test environment as the polarization curves. The typical Nyquist impedance diagrams of studied steel immersed in 3.5 wt% NaCl containing CO_2 and H_2S after different immersion time (24, 48, 96, 192 and 288 h) are shown in Fig.4. It is seen that the Nyquist plots show the properties of double capacitive semicircles. At the high frequency, the capacitive semicircle should be associated with the corrosion product film on the sample surface. However, the capacitive semicircle at low frequency should be related to the double layer capacitive and charge transfer resistance, the diameter of semicircle apparently increase as immersion time from 48 to 288 h.

Fig.5 shows the Bode plots of studied steel. The impendence modulus |Z| at high frequencies are defined a straight line with a zero slope and the phase angle remained nearby zero degrees, showing a resistance is attributed, as commonly accepted to the electrolyte resistance. The impedance modulus of studied steel at the low frequency will gradually bigger, and the peak of phase angle at low frequency increases and shifts to low frequency with the increase immersion time form 48h to 288h. The impedance modulus |Z| is biggest for studied steel after immersion 288 h, and the smallest one is after immersion 48 h. In bode plots, the two phase angle peaks are seen, so a simple equivalent circuit is used to fit the EIS data, shown in Fig.6. Table 3 lists the values of corresponding parameters. In the equivalent circuit, Rs is electrolyte resistance between the reference electrode and the working electrode. R_f is the resistance of corrosion product film. R_{ct} is the charge transfer resistance. CPE is the

constant phase element representing the double-charge layer capacitance, which is expressed as follows.

$$Z_{CPE} = \frac{1}{Y_0 (j\omega)^n} \quad (3)$$

where Y_0 is a general admittance function, j is the complex operator with $j = (-1)^{1/2}$, $\omega = 2\pi f$ is the angular frequency, $n (0 < n < 1)$ is a power. CPE_f is total surface electrode capacitance after electrode surface dispersion, $n_1 (0 < n_1 < 1)$ is dispersion effect index of CPE_f, when $n_1 = 1$, CPE_f is equivalent to the ideal capacitance, when $n_1 = 0$, CPE_f is equivalent to the ideal resistance. CPE_{dl} represents the capacitance for solution/metal surface in the corrosion hole, $n_2 (0 < n_2 < 1)$ is dispersion effect index of CPE_{dl}. The total impedance Z can be rewritten as

$$Z = R_s + \frac{1}{\frac{1}{R_f + \frac{1}{\frac{1}{Z_{CPE_{dl}}} + \frac{1}{R_{ct}}}} + \frac{1}{Z_{CPE_f}}} \quad (4)$$

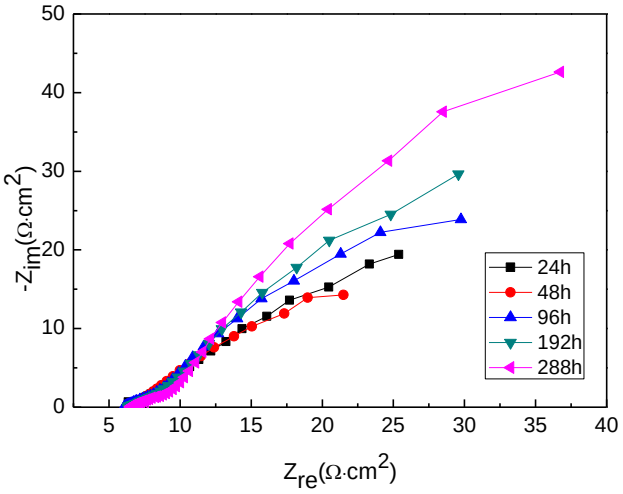

Figure 4. Nyquist plots of studied steel after immersion at different times

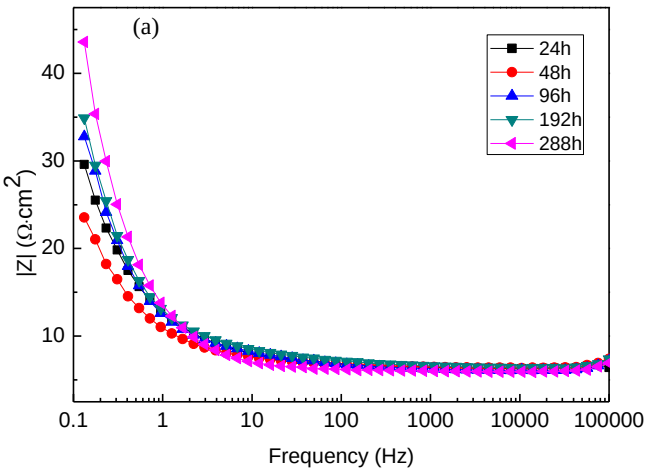

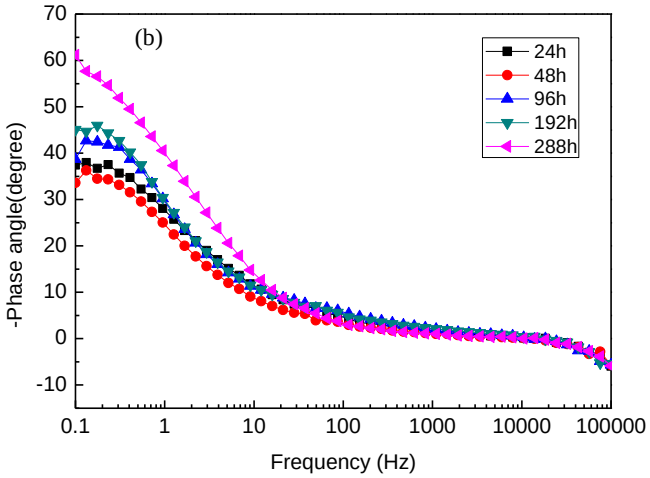

Figure 5. Bode diagrams of studied steel after immersion at different times (a) The amplitude-frequency characteristic curve (b) The phase-frequency characteristic curve

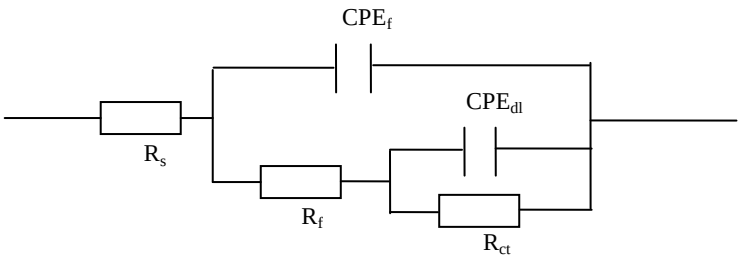

Figure 6. Electrochemical equivalent circuits for EIS fitting with two time constants

Corrosion rates are calculated by Tafel extrapolation method. The corrosion current density can be measured and can yield a corrosion rate based on the following equation [27].

$$v = 0.00327\frac{ai}{nD} \qquad (5)$$

where v is the corrosion mass rate, mm/year, a is molar mass of studied steel (g/mol), i is corrosion current density ($\mu A/cm^2$), n is valency, D is steel density.

The polarization resistance from EIS can be represented as $R_p = R_{ct} + R_f$, which has been used to explain electrochemical corrosion process [28]. According to Stern-Geary equation, we have the following equation[29].

$$i = \frac{1}{2.303R_p\left(\frac{1}{b_a} + \frac{1}{|b_c|}\right)} \qquad (6)$$

From equations (5) and (6), we get the following equation

$$v = \frac{0.00327a}{2.303nDR_p\left(\frac{1}{b_a} + \frac{1}{|b_c|}\right)} = \frac{0.00142a}{nDR_p\left(\frac{1}{b_a} + \frac{1}{|b_c|}\right)} \qquad (7)$$

We can see that there is inversely proportional relationship between corrosion rate v and polarization resistance R_p. The values of the electrochemical equivalent circuit elements for each data are given in Table 3.

The average value of R_s is about $6.5\,\Omega\cdot cm^2$ and changes a little, which will indicate each test system is at a stable state. It is seen that the resistances of corrosion product films (R_f) are relatively small and their changes are not obvious with the increase immersion time. The condition may be considered to the fact that corrosion product films are mainly made of iron sulfide, and iron sulfide is electronically conductive [21]. Therefore, the resistances of corrosion product films (R_f) are quite small. The Y_f and Y_{dl} will appear fluctuation phenomenon, and the phenomenon is more obvious, the more serious corrosion. The Y_{dl} are usually used to explain the surface roughness due to corrosion, which will lead to surface heterogeneity on the microscopic level [26].

Table 3. The Parameters of equivalent circuit for studied steel

Immersion time/hour	Sample no.	R_s ($\Omega\cdot cm^2$)	Y_f(S-sec^n/cm^2)	n_1	R_f ($\Omega\cdot cm^2$)	Y_{dl}(S-sec^n/cm^2)	n_2	R_{ct} ($\Omega\cdot cm^2$)
24	1	6.4	0.00698	0.77	10.4	0.0362	0.61	136
	2	6.4	0.00706	0.77	9.8	0.0301	0.61	159
	3	6.4	0.00758	0.77	13.6	0.0412	0.60	155
48	1	6.5	0.00249	0.99	6.7	0.0519	0.64	101
	2	6.4	0.00221	0.98	8.1	0.0603	0.65	136
	3	6.5	0.00203	0.99	8.9	0.0635	0.64	132
96	1	6.2	0.00792	0.74	20.7	0.0293	0.75	147
	2	6.2	0.00813	0.74	18.2	0.0285	0.75	181
	3	6.2	0.00799	0.72	15.6	0.0272	0.72	185
192	1	6.5	0.01175	0.69	32.4	0.0234	0.77	258
	2	6.6	0.01001	0.68	22.6	0.0197	0.76	281
	3	6.6	0.01231	0.68	40.9	0.0201	0.76	274
288	1	6.7	0.00730	0.69	39.1	0.0187	0.84	420
	2	6.7	0.00795	0.67	60.2	0.0163	0.84	416
	3	6.7	0.00742	0.60	49.3	0.0152	0.82	432

The polarization resistance R_p is used to estimate the corrosion rate of studied steel in CO_2/H_2S environment. The R_p values will increase gradually from 48 h to 288 h, the largest value is got for test steel after immersion 288 h, the smallest one is got for immersion 48 h. It is seen that the polarization resistance for studied steel after immersion 48h is obviously smaller than that after immersion 288h. The obtained result by the EIS is consistent with those obtained by weight loss and potentiodynamic polarization measurements. According to the equation (7) and Table 2, we can calculate the corrosion rate of studied steel is 1.992 2.316 1.582 1.033 0.664 mm/year after immersion time 24, 48, 96, 192 and 288 h, respectively.

The corrosion rates obtained by weight loss, potentiodynamic polarization and electrochemical impedance spectroscopy method are summarized in Fig.7. It indicates that the corrosion rates are correlated with each other, the transition point in the corrosion process is observed for immersion 48h,

the corrosion rate is biggest, the corrosion resistance is worst, with increase immersion time, the corrosion rate decrease, the corrosion resistance is well.

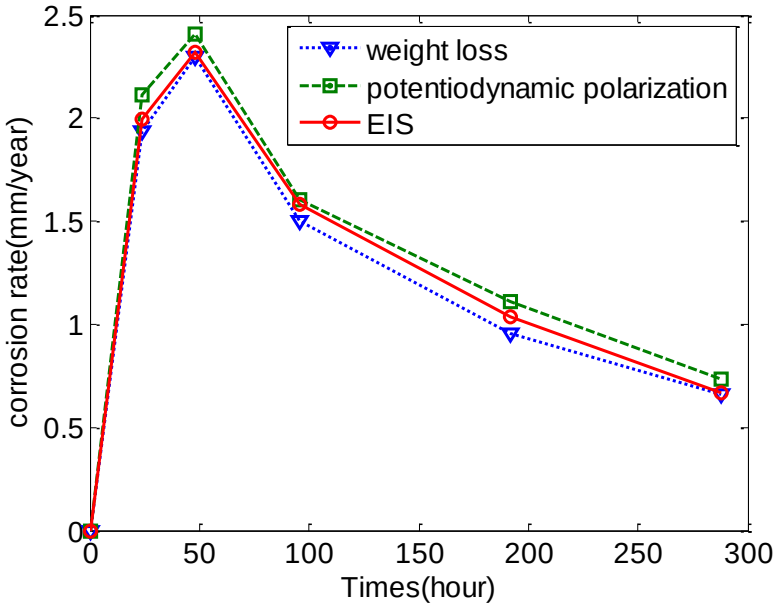

Figure 7. Comparison of corrosion rate according to weight loss test, potentiodynamic polarization and EIS measurements

3.4 Morphologies analysis of corrosion product films

3.4.1 Surface morphology

In CO_2/H_2S environment, there are various species in the solution, such as H^+, CO_3^{2-}, H_2CO_3, HS^-, S^{2-} and H_2S, the pitting corrosion of low alloy steel is very serious, the corrosion mechanism is also rather complicated [21, 30]. Fig.8 indicates the surface micrographs of experiment steel in sodium chloride solution containing CO_2 and H_2S.

Obviously, the corrosion products of studied steel after immersion 48h are loose, the corrosion solution diffuses into the inner layer and even into the substrate surface by the gaps, which will lead to a poor corrosion resistance and some localized corrosion on the surface of the substrate. Instead, with increase immersion time, the more dense corrosion products will be produced. When immersion time for 96h, the corrosion scales is relatively compact, the corrosion resistance become well, then the corrosion scales produced after immersion for 288 h are very compact, the crystal grains are more regular and dense, it can effectively protect the steel matrix, the corrosion rate is also very good. All these show that the corrosion of the studied steel after immersion 48h is more serious, the corrosion for immersion 288h is relatively well, which is in accordance with the corrosion rates described above using weight loss and electrochemical measurements.

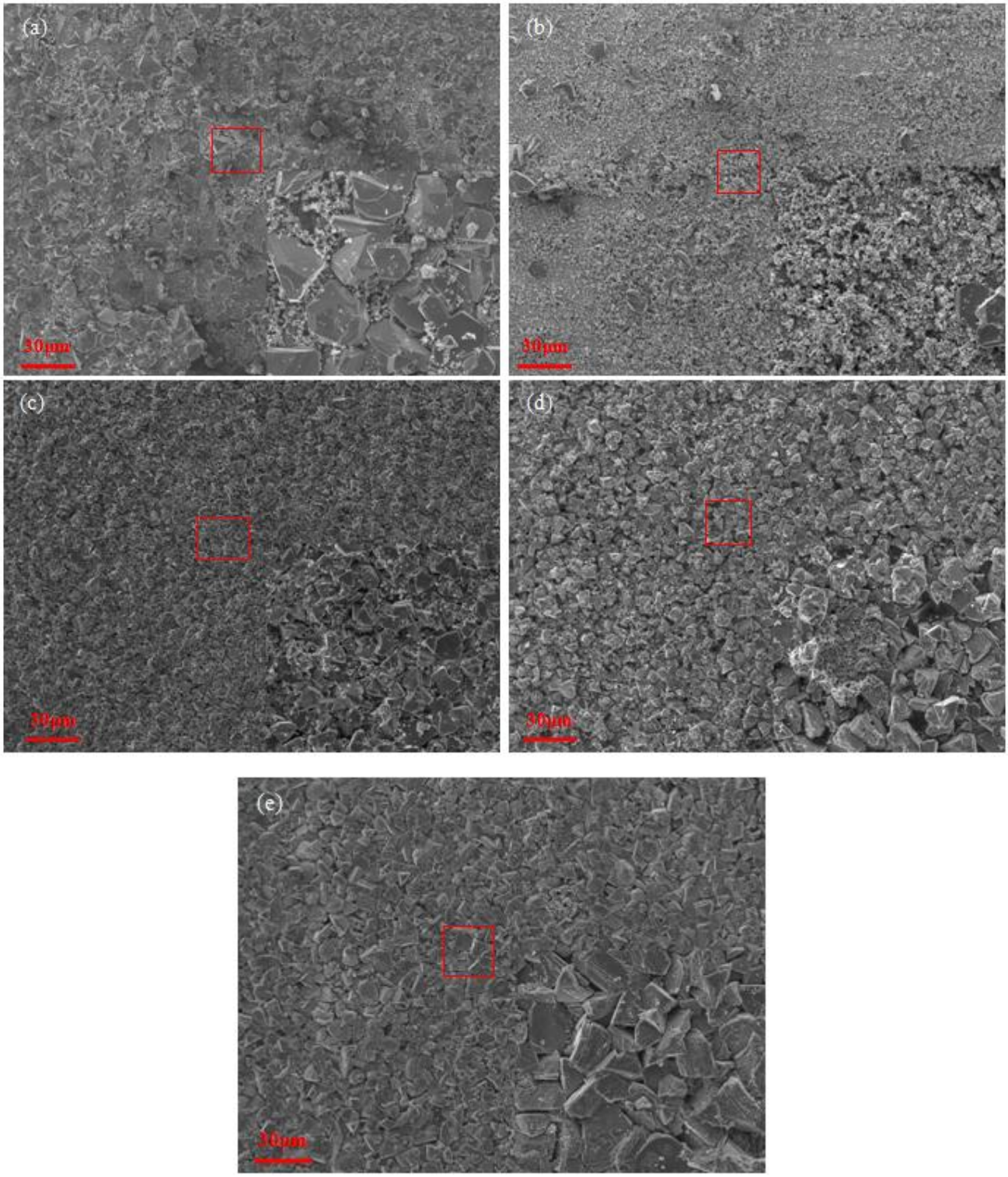

Figure 8. SEM images of corroded surface of studied steel after different immersion time: 24 h (b) 48 h (c) 96 h (d) 192h (e) 228h

Fig.9 shows the surface morphology and energy dispersive spectrometer (EDS) of studied steel after immersion 48h and 96h in sodium chloride solution containing CO_2 and H_2S. When the test steel is immersed for 24h and 48h, the primary chemical elements are the same. Typical figure for

immersion 48h is shown in Fig 9(a), we can see that the primary chemical elements of position A and B are iron, carbon, sulfur and oxygen. This indicates that the corrosion products are complexity compound containing different types of iron carbonate and iron sulfide. After immersion 96h, 192h and 288h, the primary chemical elements are the same. Typical figure for immersion 96h is shown in Fig 9(b), the primary chemical elements are iron and sulfur, carbon and oxygen is not observed. The results show the corrosion type of studied steel is mainly H_2S corrosion and the corrosion scale is mainly sulfide during the later corrosion period.

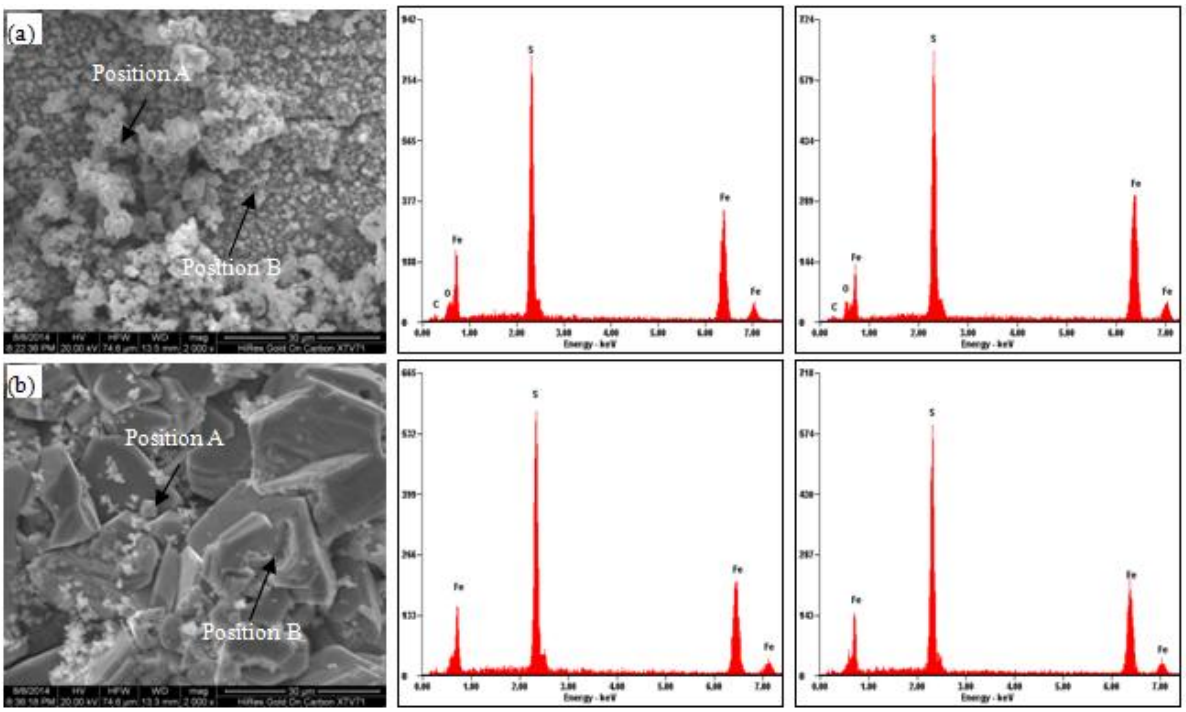

Figure 9. EDS of test steel after immersion for (a) 48h and (b) 96h

3.4.2 Cross section morphology

The cross section morphology characterization of studied steel is shown in Fig.10. From Fig.10(a), we can see that the inner layer of corrosion product film is loose ranging from 0μm to 5μm, and the outer layer is porous about 0μm to 6μm are formed on the coupon surface when immersion time is 24h, the results is consistent with surface morphology characterization showed in Fig.8(a). When immersion time reaches to 48h, the inner layer is damaged gradually, a wavy inner layer is attached on the steel substrate. With immersion time goes by from 96h to 288h, the thickness of the inner layer and outer layer increase gradually, and the structures are more compact. A denser inner layer has formed on the steel substrate, which can prevent the reaction of ions, and resist eroding further. In Fig.10(e), thickness of outer layer changes small compared to the one in Fig.10(d), but becomes more compact.

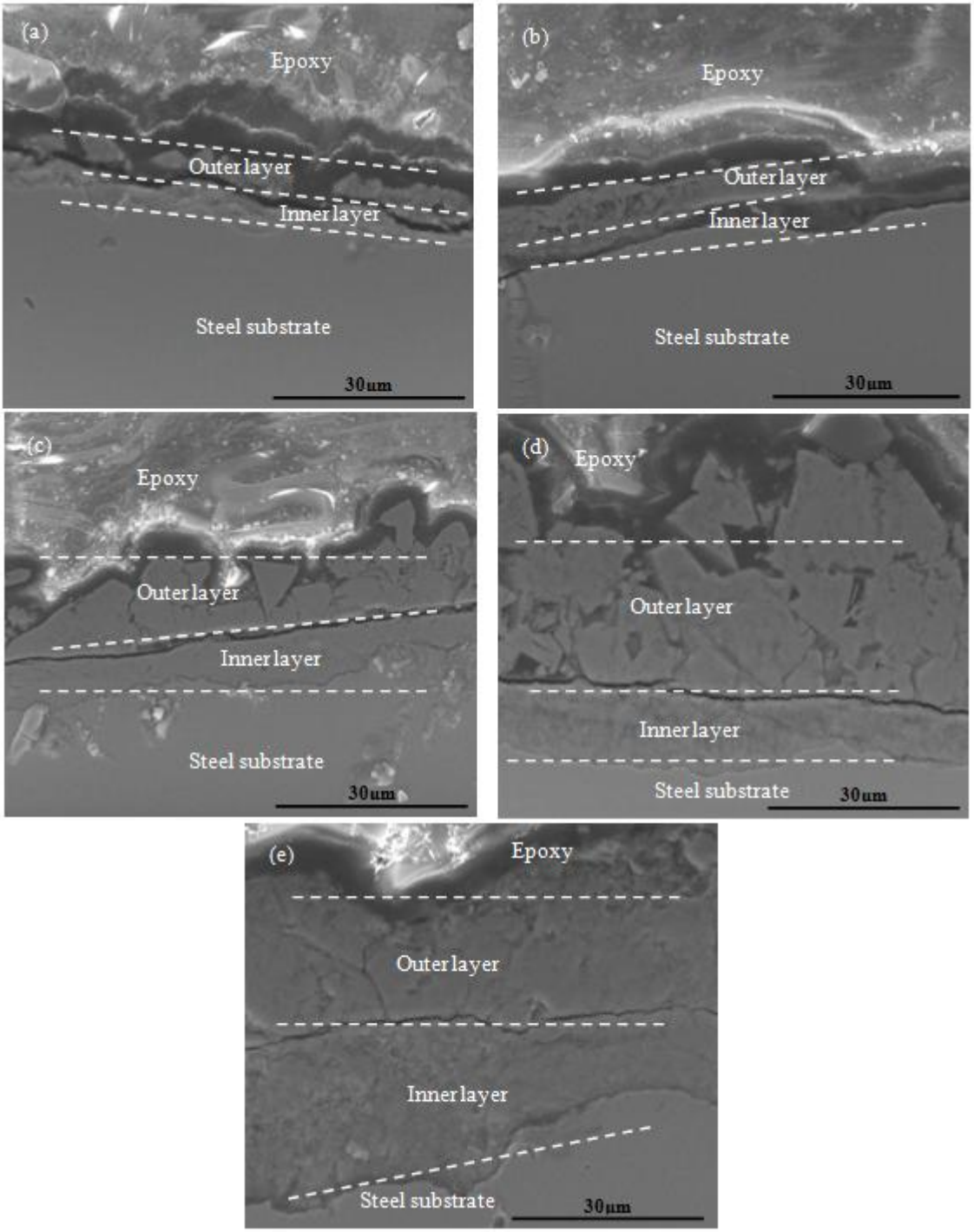

Figure 10. Cross-section morphology of studied steel after different immersion time : (a) 24 h (b) 48 h (c) 96 h (d) 192 h (e) 288 h

3.5 Corrosion phases

The XRD patterns of the corrosion scales produced at different immersion time are shown in Fig.11. It can be seen from Fig.11 (a) that the corrosion products comprise FeS (mackinawite) and $FeCO_3$ (siderite). The majority of strong peak come from FeS and some weak peaks of inhomogeneous

$FeCO_3$ occur in the spectra. When immersion time is 96h, 192h and 288h, the pattern of $FeCO_3$ is not observed. The absence of $FeCO_3$ in the corrosion product films shows that the H_2S corrosion has an important influence on the whole reaction process and iron sulfide is superior to precipitating on the steel surface compared with iron carbonate, which is in accordance with the surface morphology and EDS characterization described above. Only Fe is observed when the test steel immersed for 24h and 48h. In Fig.11(b), the number of Fe substrate peak is larger than the one in Fig.11(a). This indicates that more Fe substrate appears on the coupon surface of 48h immersion time, which will lead to the poor corrosion resistance, and these results are also related with corrosion product films. Approximately 48h later, the steel surface is covered with only FeS, as shown in Fig.11. From then on, the intensity of FeS enhances, which will increase corrosion resistance of studied steel.

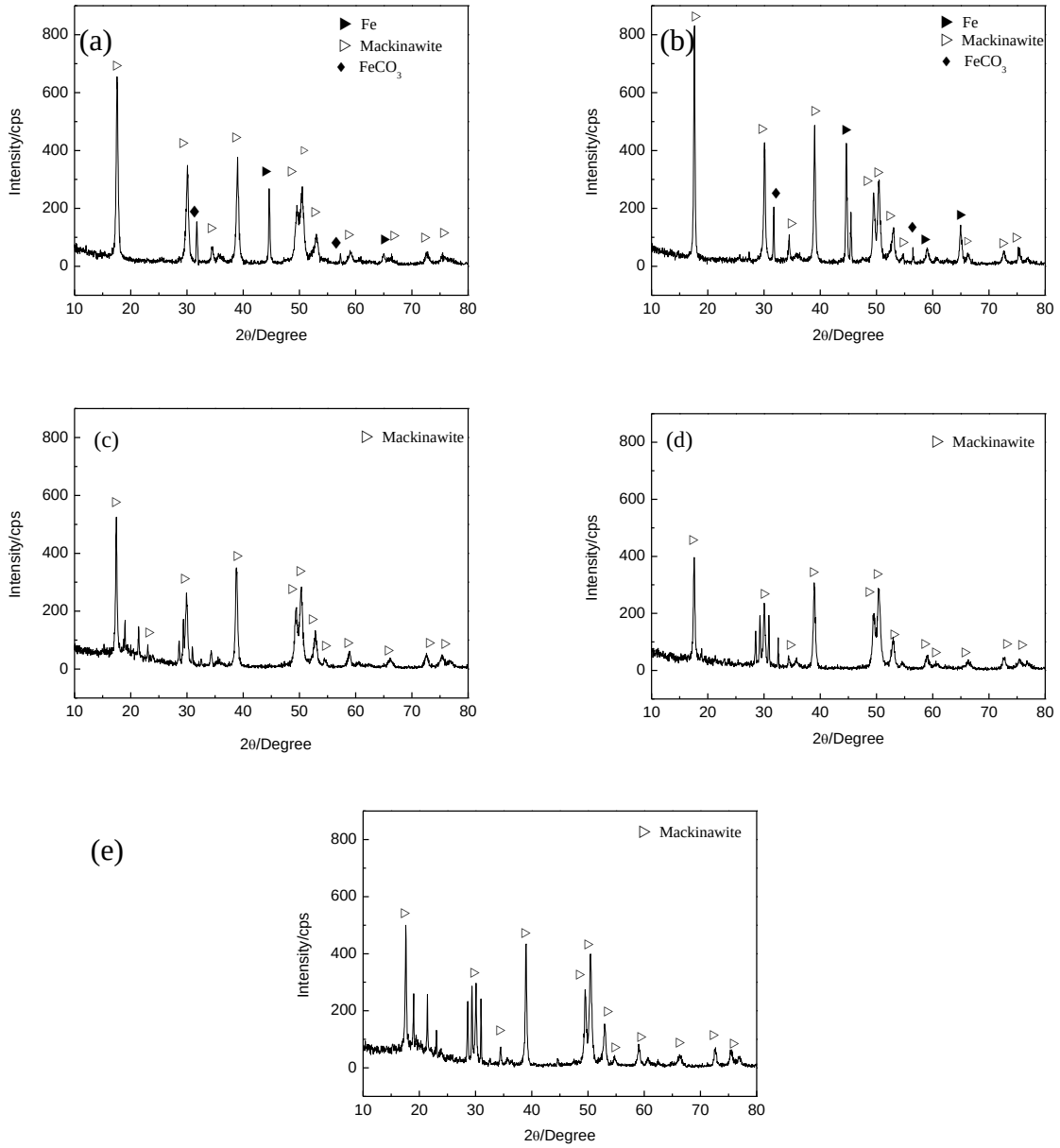

Figure 11. XRD spectra of corrosion product films of studied steel after different immersion time: (a) 24h (b) 48h (c) 96h (d) 192h (e) 228h

4. CONCLUSIONS

The corrosion mechanism of studied steel has been investigated. The corrosion properties are obtained by the experiment about weight loss and electrochemical measurements. X-ray diffraction (XRD) and energy dispersive spectrometer (EDS) are used to reveal that the major corrosion phases are FeS (mackinawite) and $FeCO_3$. A corrosion product film consisted of FeS and $FeCO_3$ appears on the surface of samples in the early stage. Later, only FeS crystal is observed, the thickness of corrosion scales will increase when immersion time range from 96 h to 288 h, the structure is more compact, the corrosion product films become more stably, and the corrosion resistance is improved.

ACKNOWLEDGEMENT
This work was financially supported by National Key Technology Research and Development Program of the Ministry of Science and Technology of China during the "12th Five-Year Plan"(Grant No. 2011BAE25B03).

References

1. L. D. Paolinelli, T. Pérez, S.N. Simison, *Corros. Sci.*, 51(2008)2456.
2. W. F. Li, Y. J. Zhou, Y. Xue, *J. Iron. Steel Res. Int.*, 19(2012)59.
3. W. He, O. Ø. Knudsen, S. Diplas, *Corros. Sci.*, 51(2009)2811.
4. X. H. Hao, J. H. Dong, J. Wei, W. Ke, C. G. Wang, X. L. Xu, Q. B. Ye, *Acta. Metall. Sin.*, 48 (2012) 534.
5. Z. C. Qiu, C. M. Xiong, Z. L. Chang, *Petrol. Explor. Dev.*, 39(2012)252.
6. B. F. M. Pot, S. D. Kapusta, R. C. John, *In: corrosion 2002, Houston*, 2002.
7. X. H. Zhao, Y. Han, Z. Q. Bai, B. Wei, *Electrochim. Acta*., 56(2011)7725.
8. L. D. Wang, H. B. Wu, Y. T. Liu, H. W. Zhang, L. F. Liu, D. Tang, *Mater. Sci. Technol.*, 21(2013)8.
9. E. Volpi, A. Olietti, M. Stefanoni, S. P. Trasatti, *J. Electroanal. Chem*., 736(2015)38.
10. Y. Zou, J. Wang, Y. Y. Zheng, *Corros. Sci.*, 53(2011)208.
11. H. W. Wang, C. Yu, S. W. Huang, *Int. J. Electrochem. Sci*., 10(2015)5827.
12. S. Marcelin, N. Pébère, S. Régnier, *Electrochim. Acta*., 87(2013)32.
13. C. Yu, P. Wang, X. H. Gao, *Int. J. Electrochem. Sci*., 10(2015)538.
14. L. W. Wang, C. W. Du, Z. Y. Liu, X. X. Zeng, X. G. Li, *Acta. Metall. Sin.*, 47(2011)1227.
15. F. Farelas, M. Galicia, B. Brown, S. Nesic, H. Castaneda, *Corros. Sci.*, 52(2010) 509.
16. J. Y. Zhu, L. N. Xu, M. X. Lu, L Zhang, W. Chang, L. H. Hu, *Int. J. Electrochem. Sci*.,10 (2015)1434.
17. N. Mundhenk, P. Huttenloch, R. Bäßler, T. Kohl, H. Steger, R. Zorn, *Corros. Sci.*, 84(2014)180.
18. J. H. Ding, L. Zhang, M. X. Lu, J. Wang, Z. B. Wen, W. H. Hao, *Appl. Surf. Sci*., 285(2014)33.
19. P. P. Bai, S. Q. Zheng, C. F. Chen, *Mater Chem Phys*, 149(2015)295.
20. M. A. Veloz, I. González, *Electrochim. Acta*., 48(2002)135.
21. G. A. Zhang, Y. Zeng, X. P. Guo, *Corros. Sci.*, 65(2012)37.
22. H. B. Wu, L. F. Liu, L. D. Wang, Y. T. Liu, *J. Iron. Steel Res. Int.*, 21(2014)76.
23. C. Yu, P. Wang, X. H. Gao, *Int. J. Electrochem. Sci*., 10(2015)6820.
24. C. Q. Ren, M. Zhu, L. Du, J. B. Chen, D. Z. Zeng, J. Y. Hu, T. H. Shi, *Int. J. Electrochem. Sci*., 10 (2015)4029.
25. F. L. Sun, X. G. Li, F. Zhang, *Acta. Metall. Sin.*, 26(2013)257.
26. L. Fan, D. H. Zhou, T. L. Wang, S. R. Li, Q. F. Wang, *Mater. Sci. Eng., A*, 590(2014)224.
27. M. N. Ilman, *Eng. Fail. Anal*., 2(2014)1.
28. A. V. C. Sobral, W Ristow, D. S. Azambuja, I. Costa, C. V. Franco, *Corros. Sci.*, 43(2001)1019.

29. E. McCafferty. *Corros. Sci.*, 47(2005)3202.
30. H. Y. Ma, X. L. Cheng, G. Q. Li, *Corros. Sci.*, 42(2000)1669.